Parametric generation of robust chaos with time-delayed feedback and modulated pump source

Alexey S. Kuznetsov [b], Sergey P. Kuznetsov [a,b,*]

[a] *Kotel'nikov's Institute of Radio-Engineering and Electronics of RAS, Zelenaya 38, Saratov 410019, Russian Federation*
[b] *Faculty of Nonlinear Processes, Saratov State University, Bolshaya Kazachya 112A, Saratov 410012, Russian Federation*

ARTICLE INFO

ABSTRACT

We consider a chaos generator composed of two parametrically coupled oscillators whose natural frequencies differ by factor of two. The system is driven by modulated pump source on the third harmonic of the basic frequency, and on each next period of pumping the excitation of the oscillator of doubled frequency is stimulated by the signal from the oscillator of the basic frequency undergoing quadratic nonlinear transformation and time delay. Using qualitative analysis and numerical results, we argue that chaotic dynamics in the system corresponds to hyperbolic strange attractor. It is a kind of Smale–Williams solenoid embedded in the infinite-dimensional state space of the stroboscopic map of the time-delayed system.

1. Introduction

According to mathematical theory of dynamical systems, chaotic attractors, possessing perfect structural stability are those relating to the class of uniformly hyperbolic attractors [1–4]. Formal examples are Smale–Williams solenoid, Plykin attractor, and a number of other mathematical constructions suggested mainly in 1960th–1970th. In such attractors, all phase trajectories are of one and the same saddle type, combining stability in a sense of approach of the nearby trajectories to the attractor and instability on the attractor resulting in chaotic nature of the dynamics. For this class, deep and comprehensive theory was developed, providing a complete mathematical description, and chaotic nature of the dynamics was proven rigorously.

Traditionally, the structural stability of dynamical phenomena is regarded as significant both for motivations of theoretical studies and for the practice [5–7]. Indeed, the structural stability implies robustness that means insensitivity of the dynamics to interferences, technical fluctuations, variation of parameters, etc. Surely, the robustness is highly desirable for chaotic dynamical systems considered in the context of their possible applications (chaos communication, random number generation, noise radar, cryptography) [8,9].

However, chaotic attractors, which normally appear in real-world systems, do not fall in the uniformly hyperbolic class [6,10–12], which looks as an obvious contradiction with the above mentioned principle of significance of structurally stable systems. This inconsistency is overcome to some extent recently after introducing a number of specially elaborated physically realizable systems with hyperbolic attractors [13–16]. A fruitful approach to their design is manipulating with phases for two or more alternately exciting and damping oscillators in such way that the phase shifts at the successive stages of activity evolve chaotically in accordance with expanding circle map [13,14].

---

* Corresponding author at: Kotel'nikov's Institute of Radio-Engineering and Electronics of RAS, Saratov Beach, Zelenaya 38, Saratov 410019, Russian Federation.
E-mail address: spkuz@rambler.ru (S.P. Kuznetsov).

The same idea may be accomplished even with a single oscillatory element by means of appropriately arranged delayed feedback providing stimulation of the excitation on each next stage of activity by signal emitted on a previous such stage [17,18]. In a frame of mathematical description, for the systems with the time delay the state space dimension appears to be formally infinite, but physically (say, in electronics, acoustics, or nonlinear optics) implementation of such setup may be easy and justifiable.

Next, as indicated e.g. in Refs. [19,20], a good opportunity for using the principle of phase manipulation is its application to systems of parametric oscillators; indeed, for them one can naturally exploit specific intrinsic relations for frequencies and phases of the involved oscillatory components.

In the present article we combine both two mentioned hints: a use of the parametric oscillations and of the time-delay feedback. On this way it appears possible to compose a simple and elegant scheme of parametric generator of robust chaos, which may be of interest from a practical point of view. Less pragmatic but more fundamental motivation is that we supply one more appealing example to a collection of physically realizable systems (not so numerous at the present moment) whose structurally stable chaotic dynamics occurs due to the uniformly hyperbolic attractors. As we suppose, it contributes to enrichment of fundamental concepts of the dynamical system theory, namely, the hyperbolic theory [1–4], with the physical content.

2. Model, principle of operation, and the basic equations

In a commonly known type of parametric generator [21], two oscillators are connected by a reactive element characterized by time-dependent oscillating coupling coefficient. The oscillation frequencies ω_1 and ω_2 and the driving pump frequency ω_3 are related by the parametric resonance condition $\omega_1 + \omega_2 = \omega_3$. Both oscillators constituting the system excite simultaneously; the instability can be saturated, say, by nonlinear damping.

Consider a system of this type schematized in Fig. 1 with the frequencies selected in such way that $\omega_2 = 2\omega_1$, $\omega_3 = 3\omega_1$ (note that the parametric resonance condition is satisfied). The oscillator of frequency ω_2 is affected by the delayed signal from the oscillator of frequency ω_1 transformed by a quadratic nonlinear element (signal squarer). By virtue of the assumed relation between the frequencies, the second harmonic of the signal is just in resonance with the driven oscillator. The pump source with the main frequency ω_3 is modulated slowly in such way that the parametric oscillations alternately arise and decay. The ratio of the period of the pump modulation T and the time delay in the feedback loop τ must be chosen in such way that each next excitation of the system is stimulated by the signal emitted at the previous stage of activity (particularly, $\tau = T/2$ is appropriate). Hence, the oscillation phase is doubled after each next excitation transfer. As a result, the system generates, with the modulation period, a sequence of pulses whose carrier phase chaotically varies from pulse to pulse. The chaotic dynamics in this mode of operation is supposed to be associated with a uniformly hyperbolic attractor; for the map governing transformation of the system state over a modulation period this is a kind of Smale–Williams solenoid [6,1,2,15].

To simulate the proposed device, consider a model set of delay-differential equations

$$
\begin{aligned}
\ddot{x}_1 + \omega_1^2 x_1 &= \kappa x_2 f(t) \sin \omega_3 t - \alpha_1 \dot{x}_1 - \beta_1 \dot{x}_1^3, \\
\ddot{x}_2 + \omega_2^2 x_2 &= \kappa x_1 f(t) \sin \omega_3 t - \alpha_2 \dot{x}_2 - \beta_2 \dot{x}_2^3 + \varepsilon x_1^2(t - \tau),
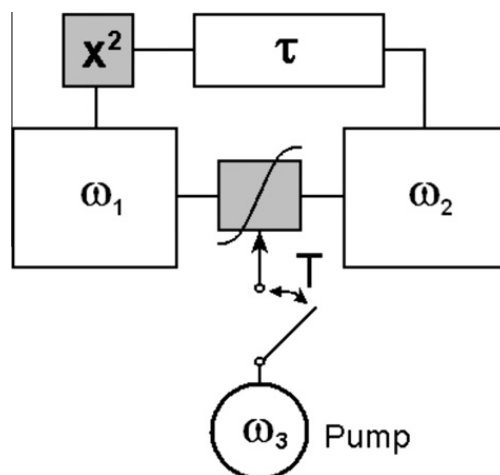\end{aligned}
\tag{1}
$$

Fig. 1. Block diagram of the parametric chaos generator. Blocks labeled as ω_1 and ω_2 represent oscillators with these frequencies; the block labeled with a waveform is a reactive element characterized by the coupling parameter oscillating due to the pump source with the carrier frequency ω_3, and the block marked with x^2 is the quadratic nonlinear element (the signal squarer).

where x_1 and x_2 are the generalized coordinates of two oscillators. Parameter κ quantifies the pump intensity, and the function $f(t)$ determines the slowly varying periodic amplitude of the pump. Concretely, throughout the present article we set

$$f(t) = \cos^2(\pi t/T). \tag{2}$$

Parameter ε is the transmission coefficient for the squared signal of the first oscillator in the feedback loop with the time delay τ. Parameters $\alpha_{1,2}$ and $\beta_{1,2}$ characterize, respectively, linear and nonlinear damping of the oscillators; the last is needed for saturation of the parametric instability and for existence of the attractor. To get perfectly periodic coefficients in the equations, we set the modulation period to be equal to a multiple of the high-frequency carrier period: $T = 2\pi N/\omega_3$, where N is an integer.

When $N \gg 1$, the method of slow amplitudes can be used for description of the dynamics [7,21–23]. To apply this method, we set

$$\begin{aligned}
x_j &= A_j e^{i\omega_j t} + A_j^* e^{-i\omega_j t}, \\
\dot{x}_j &= i\omega_j A_j e^{i\omega_j t} - i\omega_j A_j^* e^{-i\omega_j t}, \quad j = 1,2,
\end{aligned} \tag{3}$$

where $A_1(t)$ and $A_2(t)$ are slowly varying complex functions of time subjected the conditions

$$\dot{A}_j e^{i\omega_j t} + \dot{A}_j^* e^{-i\omega_j t} = 0, \quad j = 1,2. \tag{4}$$

Substituting these relations into (1), multiplying the equations for A_1 by $e^{-i\omega_1 t}$ and for A_2 by $e^{-i\omega_2 t}$, averaging the resulting equations over the carrier period, and using the assumed relation between the frequencies $\omega_{1,2,3}$, we obtain

$$\begin{aligned}
\dot{A}_1 &= -\frac{\kappa}{4\omega_1} f(t) A_2^* - \frac{1}{2}\alpha_1 A_1 - \frac{3}{2}\omega_1^2 \beta_1 A_1 |A_1|^2, \\
\dot{A}_2 &= -\frac{\kappa}{4\omega_2} f(t) A_1^* - \frac{1}{2}\alpha_2 A_2 - \frac{3}{2}\omega_2^2 \beta_2 A_2 |A_2|^2 - i\frac{\varepsilon}{2\omega_2} e^{-2i\omega_1 \tau} A_1^2(t - \tau).
\end{aligned} \tag{5}$$

In the case $\varepsilon = 0$, $\alpha_{1,2} = \beta_{1,2} = 0$, and $f(t) \equiv 1$, the equations are solvable. The general solution is $A_1 = C_+ e^{\kappa t/4\sqrt{\omega_1 \omega_2}} + C_- e^{-\kappa t/4\sqrt{\omega_1 \omega_2}}$, $A_2 = -\sqrt{\omega_2/\omega_1}(C_+^* e^{\kappa t/4\sqrt{\omega_1 \omega_2}} + C_-^* e^{-\kappa t/4\sqrt{\omega_1 \omega_2}})$, where $C_+ = Re^{i\varphi}$ and C_- are complex constants determined by initial conditions. Since the second terms decay, the long-time asymptotic expressions are $A_1 \cong R \cdot e^{i\varphi} e^{\kappa t/4\sqrt{\omega_1 \omega_2}}$ and $A_2 \cong -\sqrt{\omega_2/\omega_1} R \cdot e^{-i\varphi} e^{\kappa t/4\sqrt{\omega_1 \omega_2}}$, which correspond to $x_1 \cong 2R \cdot e^{\kappa t/4\sqrt{\omega_1 \omega_2}} \cos(\omega_1 t + \varphi)$ and $x_2 \cong -2R \cdot \sqrt{\omega_2/\omega_1} e^{\kappa t/4\sqrt{\omega_1 \omega_2}} \cos(\omega_2 t - \varphi)$. Thus, the phase shifts for the parametrically excited oscillators at the frequencies ω_1 and ω_2 are characterized by one and the same constant φ depending on initial conditions. When the nonlinear damping is taken into account, the oscillation amplitudes saturate, yet the phase relation is preserved.

Now, consider qualitatively a mode of operation when the pump is periodically switched on and off in the system with $\varepsilon \neq 0$ and with damping. In this case the oscillator of frequency $\omega_2 = 2\omega_1$ is excited by the second harmonic of the signal, which is emitted on the previous stage of activity from the oscillator of frequency ω_1. It is produced by a signal squarer and transmitted through the delayed feedback loop (with a correctly chosen relation of the delay time and the modulation period). The phase shift for this harmonic is 2φ (as seen from the identity $\cos^2(\omega_1 t + \varphi) = \cos 2(\omega_1 t + \varphi)$+off-resonant term). Supposing that the rest oscillations from the previous epoch of excitation have time to decay till the beginning of the next activity stage, the doubled phase shift in the second harmonic will be passed to the oscillator of frequency ω_2 as it stimulates its excitation. Thus, on the current stage of activity we will have $\varphi_{new} = -2\varphi + \text{const} \ (mod 2\pi)$. For the cyclic variable φ it is a Bernoulli-type expanding circle map with chaotic dynamics characterized by a positive Lyapunov exponent $\Lambda = \ln 2 \approx 0.693$.

Dealing with the non-autonomous time-delayed system, it is appropriate to consider a construction analogous to the stroboscopic Poincaré map in periodically non-autonomous ordinary differential equations [24,25,15]. The description may be formulated in terms of a stroboscopic functional map

$$\mathbf{X}_{n+1}(t) = \mathbf{F}[\mathbf{X}_n(t)]. \tag{6}$$

Here the vector functions $\mathbf{X}_n(t)$ are defined on an interval of length τ as $\mathbf{X}_n(t) = \mathbf{x}(t + nT)$, where $\mathbf{x}(t)$ is a vector of original variables $\mathbf{x}(t) = \{x_1(t), \dot{x}_1(t), x_2(t), \dot{x}_2(t)\}$ or $\mathbf{x}(t) = \{\text{Re}A_1, \text{Im}A_1, \text{Re}A_2, \text{Im}A_2\}$.

In the state space of our system, which is the space of the functions $\mathbf{X}_n(t)$, one can introduce a cyclic coordinate φ, which undergoes, as explained, the doubling transformation with each iteration of the map while in all other directions of this space compression of the phase volume takes place. (It follows from computations of the Lyapunov exponents discussed in the next section.) It suggests that the attractor of the map (6) is a kind of Smale–Williams solenoid embedded in the infinite-dimensional state space of this map.

3. Chaotic dynamics of the system. Numerical simulation

We simulate dynamics of the system setting $\omega_1 = 2\pi$, $\omega_2 = 4\pi$, and $\omega_3 = 6\pi$ (in other words, accept a convention to measure time in units of a natural period of the first oscillator). Fig. 2 shows samples of waveforms x_1 and x_2 obtained from
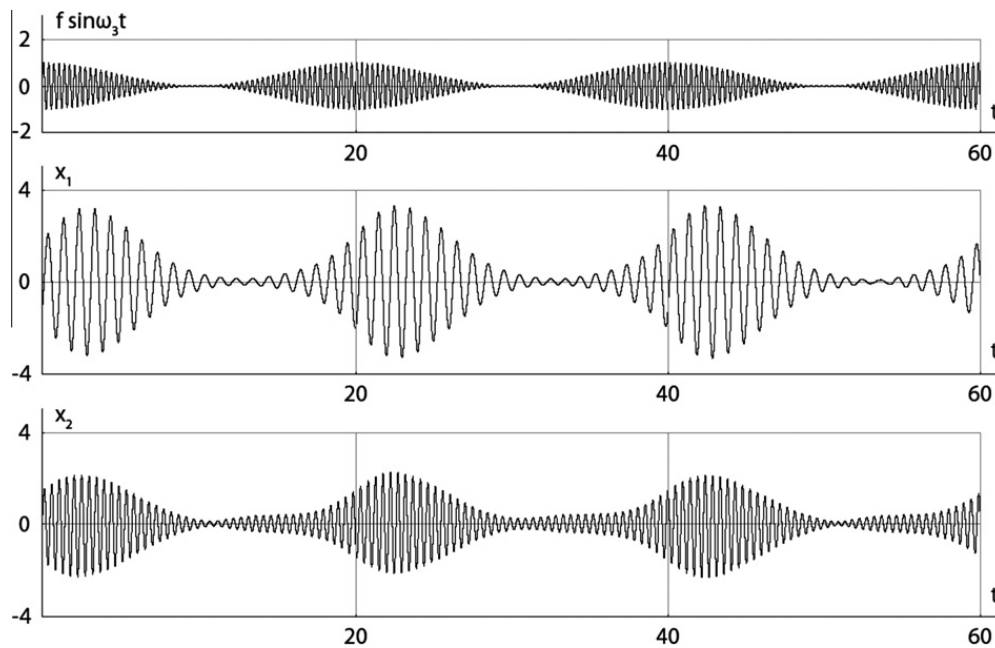
Fig. 2. Plots obtained from computing equation (1) at $\omega_1 = 2\pi$, $\omega_2 = 4\pi$, and $\omega_3 = 6\pi$ with parameter values (7): (a) driving signal; (b), (c) waveforms for the first and the second oscillator in the system.

numerical integration for the model (1) using the second-order finite-difference method adopted for the delay-differential equations. The plots relate to a sustained regime (transients are excluded). The parameter values are

$$T = 20, \quad \tau = 10, \quad \kappa = 35, \quad \varepsilon = 1, \quad \alpha_{1,2} = 1, \quad \beta_{1,2} = 0.0015. \qquad (7)$$

Observe that the waveform of each oscillator is a train of pulses following with the pump modulation period, and the carrier frequencies correspond to the respective natural frequencies. However, the waveforms are not strictly periodic: the carrier phases vary irregularly from pulse to pulse. Fig. 3 illustrates nature of the long-time dynamics of the system, which is not so obvious from the previous diagram. Here we present graphically the time series for the coordinate variable relating to the first oscillator x; it is sampled with the time step equal to the modulation period at the instants $t_n = nT$. Obviously, a chaotic behavior is observed from the diagram.

It occurs that the amplitude equation (5) deliver remarkably good description for the dynamics, at least in the parameter range we consider here. Fig. 4 shows plots for amplitudes and phases versus time obtained from numerical solution of the averaged equation (5) at the parameter values assigned in accordance with (7).

Fig. 5 shows the empirically obtained maps for the phases in successive epochs of activity. Here, the abscissa and the ordinate correspond to the phases at $t_n = nT$ and at t_{n+1}. Plots in Fig. 5a and b are obtained by computing equations (1) and (5), respectively, and calculating the phases as $\varphi_n = \arg[x_1(t_n) + \dot{x}_1(t_n)/i\omega_1]$ and $\varphi_n = \arg A_1(t_n)$. Note that the phase is well defined only within a time interval of active stage (when the output amplitude does not approach zero). As seen from Fig. 4, as φ_n varies from 0 to 2π, the phase φ_{n+1} rounds the unit circle twice in the opposite direction; i.e., the map is topologically equivalent to the Bernoulli-type map $\varphi_{new} = -2\varphi + \text{const} \ (mod 2\pi)$. The minor splitting of the branches on the plots may be regarded as unimportant and can be neglected.

Fig. 6 shows phase portraits of the attractor in the Poincaré section obtained by projection onto the phase plane of oscillator 1. Panel (a) corresponds to the original model (1) while the picture on the panel (b) is obtained from the amplitude equation (5). Both diagrams look similar; in particular, transversal fractal structure is visible that is a characteristic feature
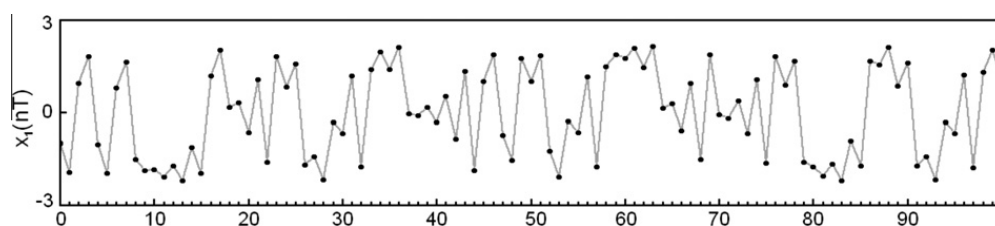

Fig. 3. Chaotic time series for the variable x_1 sampled from data of numerical integration of Eq. (1) at the time instants $t_n = nT$; the parameters are the same as indicated in the caption of the previous figure. (The gray lines do not reflect the intermediate time dependencies; they are shown only to indicate clearly the mutual dispositions of the dots on the diagram.)
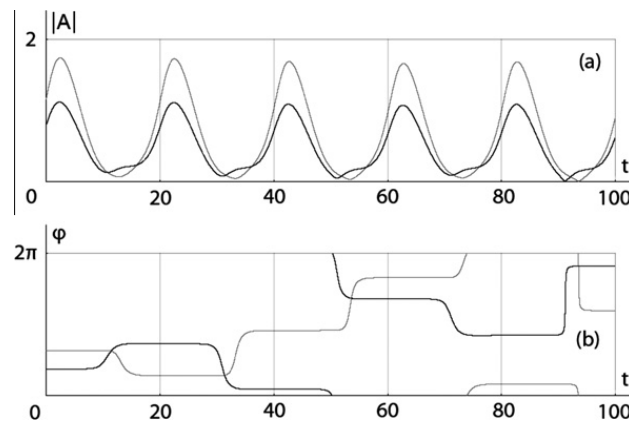
Fig. 4. Plots obtained from computing amplitude equation (5) with the same parameter values as in Fig. 2: (a) amplitudes of oscillators 1 (gray) and 2 (black) versus time, and their phases evaluated as the arguments of the complex amplitudes $A_{1,2}$ (b).
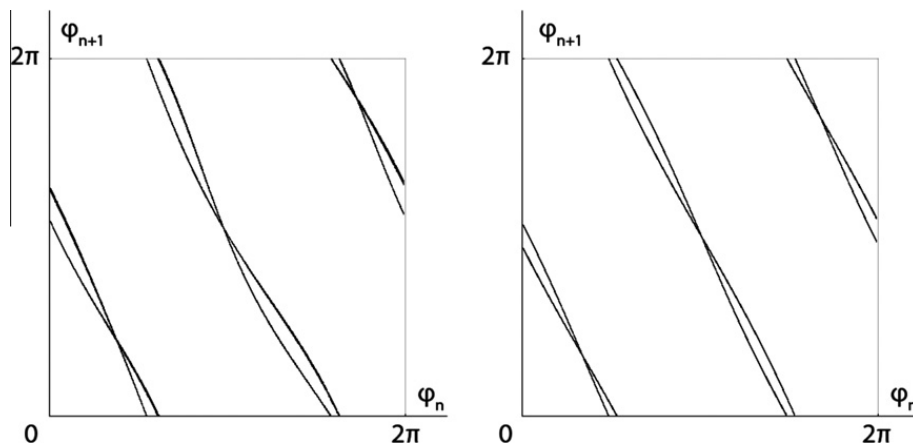

Fig. 5. Empirical iteration maps for the phases at successive stages of activity obtained in computations from Eq. (1) with $\omega_1 = 2\pi, \omega_2 = 4\pi$, and $\omega_3 = 6\pi$(a), and from Eq. (5) (b) at the parameter values (7).
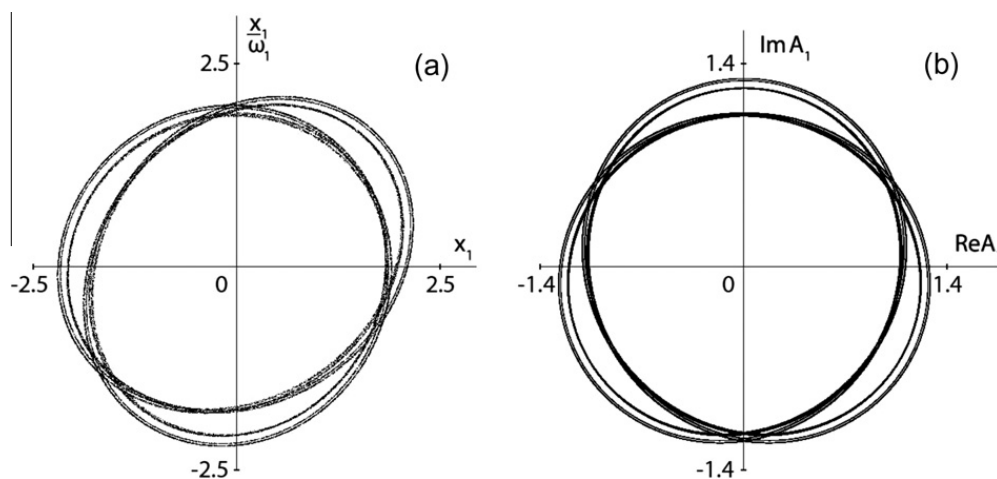

Fig. 6. Stroboscopic portraits of the attractor in projection onto the phase plane of the oscillator 1 (a) for the original model (1) with $\omega_1 = 2\pi$, $\omega_2 = 4\pi$, $\omega_3 = 6\pi$ and (b) for the amplitude equation (5) at parameter values (7).

of the Smale–Williams solenoid. (Some visible relative turn of one and other pictures may be related with the fact that in derivation of Eq. (5) we neglect slow variation of the pump amplitude when undertake the averaging over a period of fast oscillations.)

Table 1
Four larger Lyapunov exponents computed at the parameters (7).

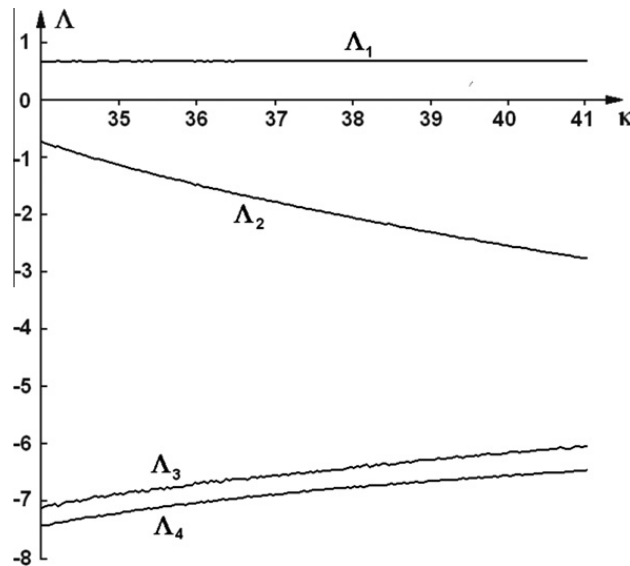|	Λ_1	Λ_2	Λ_3	Λ_4
System (1), $\omega_1 = 2\pi$, $\omega_2 = 4\pi$, $\omega_3 = 6\pi$	0.6805	−1.095	−6.798	−7.090
System (5)	0.6819	−1.162	−6.752	−7.064

Fig. 7. The largest four Lyapunov exponents plotted versus parameter κ as evaluated numerically for the system (5); the parameters are assigned according to (7).

Quantitative evidence of chaotic behavior may be obtained by calculating Lyapunov exponents. Formally, in the time-delayed system the spectrum of the Lyapunov exponents contains an infinite number of them, but practically it is reasonable to account a bounded number K of the Lyapunov exponents sufficient to evaluate the Kaplan-Yorke dimension. To compute the Lyapunov spectrum, a version of the Benettin algorithm was applied adopted for the delay-differential equations [26,27]. Eq. (1) are computed simultaneously with K sets of variation equations for the perturbations (marked by tilde):

$$\ddot{\tilde{x}}_1 + \omega_1^2 \tilde{x}_1 = \kappa \tilde{x}_2 f(t) \sin \omega_3 t - \alpha_1 \dot{\tilde{x}}_1 - 3\beta_1 \dot{x}_1^2 \dot{\tilde{x}}_1,$$
$$\ddot{\tilde{x}}_2 + \omega_2^2 \tilde{x}_2 = \kappa \tilde{x}_1 f(t) \sin \omega_3 t - \alpha_2 \dot{\tilde{x}}_2 - 3\beta_2 \dot{x}_2^2 \dot{\tilde{x}}_2 + 2\varepsilon x_1(t-\tau)\dot{\tilde{x}}_1(t-\tau) + 2\varepsilon \tilde{x}_1(t-\tau)\dot{x}_1(t-\tau),$$

(8)

or, in the case of description in terms of slow amplitudes with Eq. (5),

$$\dot{\tilde{A}}_1 = -\frac{\kappa}{4\omega_1} f(t)\tilde{A}_2^* - \frac{1}{2}\alpha_1 \tilde{A}_1 - \frac{3}{2}\omega_1^2 \beta_1 A_1^2 \tilde{A}_1^* - 3\omega_1^2 \beta_1 A_1^* A_1 \tilde{A}_1,$$
$$\dot{\tilde{A}}_2 = -\frac{\kappa}{4\omega_2} f(t)\tilde{A}_1^* - \frac{1}{2}\alpha_2 \tilde{A}_2 - \frac{3}{2}\omega_2^2 \beta_2 A_2^2 \tilde{A}_2^* - 3\omega_2^2 \beta_2 A_2^* A_2 \tilde{A}_2 - i\frac{\varepsilon}{\omega_2} A_1(t-\tau)\tilde{A}_1(t-\tau).$$

(9)

As each next modulation period comes to the end, the Gram–Schmidt orthonormalization process is applied to the perturbation vectors $\tilde{\mathbf{X}}_n(t)$ (see the map (6) and supplied explanations). The Lyapunov exponents are evaluated by averaging the growth rates for sums of logarithms of norms of the perturbation vectors after orthogonalizing, but before normalizing.

The larger Lyapunov exponents calculated for the attractor of the stroboscopic map of the system (1) and of the amplitude equation (5) are presented in Table 1. Observe good correspondence of the data for the original model and for the amplitude equations. Note that the largest exponent Λ_1, is close to the expected value $\ln 2 \approx 0.693$ corresponding to the Bernoulli-type expanding map. Other Lyapunov exponents are negative; it means compression along all directions in the state space beside the one associated with the cyclic coordinate φ and with the exponent Λ_1. The Kaplan-Yorke dimension evaluated from the spectrum of the Lyapunov exponents $D = 1 + \Lambda_1/|\Lambda_2|$ is about 1.6 for both models.

Fig. 7 shows the Lyapunov exponents obtained numerically for the amplitude equation (5) versus parameter κ (other parameters are fixed, see (7)). Observe that the positive Lyapunov exponent is practically constant in the parameter interval and is close to the value $\ln 2$. Other exponents are negative and vary slightly depending on the parameter; visually the dependence is smooth (up to numerical accuracy). Such kind of the behavior of the Lyapunov exponents indicates robust nature of the dynamics: chaos occupies the whole parameter range, and no windows of periodicity occur inside it.

4. Conclusion

We propose a scheme of parametric chaos generator composed of two coupled oscillators excited by periodically modulated pump source and with quadratic nonlinear delayed feedback. The system generates oscillations in the form of a sequence of pulses in which the carrier phase varies chaotically. Basing on qualitative analysis and data of computer simulation we conjecture that a hyperbolic strange attractor occurs in the system, which is a kind of the Smale–Williams solenoid embedded in the infinite-dimensional state space of the respective stroboscopic mapping.

Since the used approaches and combinations of elements are common e.g. in electronics, acoustics, nonlinear optics (parametric coupling, pumping, modulation) [21,28–30], the implementation of devices based on the suggested scheme seems quite feasible. Such systems can be of interest as chaos generators, including their application in hidden communication schemes [31,32]. A considerable practical advantage of systems with hyperbolic attractors is their structural stability, which implies insensitivity of the properties of generated chaos to variations of parameters and of characteristics of elements constituting the device, to technical fluctuations, and so on. Also, a feature of the system is that chaos manifests itself in a random variation of the carrier phases in the sequence of pulses. In chaos based communication systems, it may be an advantage for signal transmission in a communication channel that will be much less sensitive to noises, losses, and distortions than in other schemes (in some analogy with the well-known advantage of frequency or phase modulation compared to amplitude modulation in traditional radio-communication).

Acknowledgment

References

[1] Anosov DV, Gould GG, Aranson SK, Grines VZ, Plykin RV, Safonov AV, et al. Dynamical systems IX: dynamical systems with hyperbolic behaviour. Encyclopaedia of mathematical sciences, vol. 9. Springer; 1995.
[2] Smale S. Differentiable dynamical systems. Bull Amer Math Soc (NS) 1967;73:747–817.
[3] Williams RF. Expanding attractors. Publications Mathématiques de l'I.H.É.S. 1974;43:169–203.
[4] Plykin RV. Sources and sinks of A-diffeomorphisms of surfaces. Math USSR Sb 1974;23(2):233–53.
[5] Andronov AA, Vitt AA, Khaĭkin SĖ. Theory of oscillators. Pergamon Press; 1966.
[6] Shilnikov L. Mathematical problems of nonlinear dynamics: a tutorial. Int J Bifurcation Chaos 1997;7:1353–2001.
[7] Rabinovich MI, Trubetskov DI. Oscillations and waves: in linear and nonlinear systems. Kluwer Acad Pub; 1989.
[8] Banerjee S, Yorke JA, Grebogi C. Robust chaos. Phys Rev Lett 1998;80:3049–52.
[9] Zeraoulia E, Sprott JC. Robust chaos and its applications. World Scientific; 2011.
[10] Bonatti C, Diaz LJ, Viana M. Dynamics beyond uniform hyperbolicity. A global geometric and probobalistic perspective. Encyclopedia of mathematical sciences, vol. 102. Berlin: Springer; 2005.
[11] Anishchenko VS. Nonlinear dynamics of chaotic and stochastic systems: tutorial and modern developments. Berlin: Springer; 2002.
[12] Loskutov A. Fascination of chaos. Phys Usp 2010;53:1257–80.
[13] Kuznetsov SP. Example of a physical system with a hyperbolic attractor of the Smale–Williams type. Phys Rev Lett 2005;95:144101.
[14] Kuznetsov SP, Pikovsky A. Autonomous coupled oscillators with hyperbolic strange attractors. Physica D 2007;232:87–102.
[15] Kuznetsov SP. Hyperbolic chaos: a physicist's view. Beijing: Higher Education Press and Berlin: Springer; 2012.
[16] Kuznetsov SP. Dynamical chaos and uniformly hyperbolic attractors: from mathematics to physics. Phys Usp 2011;54:119–44.
[17] Kuznetsov SP, Ponomarenko VI. Realization of a strange attractor of the Smale–Williams type in a radiotechnical delay-feedback oscillator. Tech Phys Lett 2008;34:771–3.
[18] Kuznetsov SP, Pikovsky A. Hyperbolic chaos in the phase dynamics of a Q-switched oscillator with delayed nonlinear feedbacks. Europhys Lett 2008;84:10013.
[19] Kuznetsov SP. On feasibility of a parametric generator of hyperbolic chaos. JETP 2008;106:380–7.
[20] Kuznetsov AS, Kuznetsov SP, Sataev IR. Parametric generator of hyperbolic chaos based on two coupled oscillators with nonlinear dissipation. Tech Phys 2010;55:1707–15.
[21] Louisell WH. Coupled mode and paramagnetic electronics. New York: Wiley; 1960.
[22] Nayfeh AH. Perturbation methods. Wiley; 2000.
[23] Grebenikov E, Mitropolsky YA, Ryabov YA. Asymptotic methods in resonance analytical dynamics. CRC Press; 2004.
[24] Kuznetsov SP. Complex dynamics of oscillators with delayed feedback. Radiophys Quantum Electron 1982;25:996–1009.
[25] Giacomelli G, Politi A. Relationship between delayed and spatially extended dynamical systems. Phys Rev Lett 1996;76:2686–9.
[26] Farmer JD. Chaotic attractors of an infinite-dimensional dynamical system. Physica D 1982;4:366–93.
[27] Balyakin AA, Ryskin NM. Features of computation of spectrum of Lyapunov exponents in distributed self-oscillatory systems with delayed feedback. Izvestija VUZov – Applied Nonlinear Dynamics (Saratov) 2007;15(6):3–21 (in Russian).
[28] Akhmanov SA, Khokhlov RV. Parametric amplifiers and generators of light. Sov Phys Usp 1966;9(2):210–22.
[29] Piskarskas A, Stabinis A, Yankauskas A. Phase phenomena in parametric amplifiers and generators of ultrashort light pulses. Sov Phys Usp 1986;29:869–79.
[30] Gurbatov SN, Rudenko OV, Saichev AI. Waves and structures in nonlinear nondispersive media. General theory and applications to nonlinear acoustics. Beijing: Higher Education Press and Berlin: Springer; 2012.
[31] Yang T. A survey of chaotic secure communication systems. Int J Comput Cognition 2004;2(2):81–130.
[32] Koronovskii AA, Moskalenko OI, Hramov AE. On the use of chaotic synchronization for secure communication. Physics – Uspekhi 2009;52:1213–38.